

Fabrication and Characterization of Large, Perfectly Periodic Arrays of Metallic Nanocups

H. G. Svavarsson · J. W. Yoon · M. Shokooh-Saremi ·
S. H. Song · R. Magnusson

Received: 25 December 2011 / Accepted: 5 March 2012 / Published online: 27 March 2012
© Springer Science+Business Media, LLC 2012

Abstract Fabrication of plasmonic resonance devices composed of large arrays of highly ordered gold nanocups is presented. The nanostructures are generated from periodic photoresist templates created by interference lithography and subsequent reflow, deposition, and dislodging. The nanocups are hemispherical in shape and arranged in both rectangular and hexagonal arrays with periods of ~500 nm. Their ability to support surface plasmonic resonances is manifested experimentally by reflectance spectroscopy. Theoretical modeling to ascertain the plasmonic spectra of these nanostructures is performed. The computed spectra of the rectangular structure are in qualitative agreement with the measurements. A weaker correlation observed for the hexagonal structure is explained by its more intricate symmetry which complicates the spectral response.

Keywords Nanocups · Periodic arrays · Nano-indented films · Plasmonics · Hexagonal arrays · Rectangular arrays

Introduction

Isolated or arrayed nanoparticles with subwavelength dimensions can be designed to manipulate the photonic response of materials in fundamental ways. Surface plasmon polaritons (SPPs) propagating along periodic interfaces as well as localized photonic resonances are of interest in application areas such as metamaterials, surface-enhanced Raman scattering (SERS), and sensors [1]. Whereas the nanostructures can have various forms, many researchers have endeavored to attain spherical or cup-like shapes. Such nanocups can be imbued with plasmonic properties that provide, for example, magneto-inductive coupling between the particle and the incident light. A common approach to produce nanocups is to use a spherical particle as a template. With rather general use in mind, Love et al. [2] applied spherical silica colloids ~100–500 nm in diameter and metal deposition and then dissolved the template to obtain half-shells with a wall thickness of few nanometers. TiO₂ nanobowls with a diameter of 500 nm have also been prepared by arranging self-assembled monolayers of polystyrene spheres on a flat substrate followed by TiO₂ atomic layer deposition, ion beam milling, and etching [3]. Similar methods have been applied to fabricate gold (Au) [4], Ag [5], and Ni [6] nanocup arrays on monolayer polystyrene spheres. With more specific use in mind, Au particles with crescent moon cross-sections for field enhancements for SERS [7] and subwavelength plasmonic nanocups for metamaterial applications have furthermore been fabricated [8].

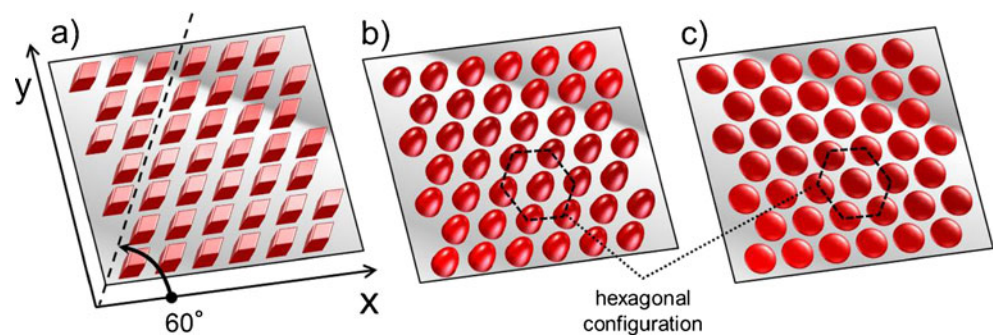
H. G. Svavarsson (✉)
School of Science and Engineering, Reykjavik University,
Menntavegur 1,
101 Reykjavik, Iceland
e-mail: halldorsv@ru.is
URL: www.ru.is/halldorsv

J. W. Yoon · M. Shokooh-Saremi · R. Magnusson
Department of Electrical Engineering,
University of Texas at Arlington,
Box 19016, Arlington, TX 76019, USA

M. Shokooh-Saremi
Department of Electrical Engineering,
Ferdowsi University of Mashhad,
Mashhad, Iran

S. H. Song
Department of Physics, Hanyang University,
17 Haengdang-dong, Seongdong-gu,
Seoul 133-791, Republic of Korea

Fig. 1 Schematic expression of the PR structures after exposure to UV interference patterns at 0° and 60° angles and subsequent development. **a** Prior to reflow. **b** After reflow for 15 s. **c** After reflow for 20 s



In a recent paper [9], we introduced a large-scale fabrication method for strictly regular arrays of gold indentations with a rectangular array configuration enabled by inverse templates. In the present contribution, we build on the method's potential and fabricate arrays of highly spherical nanocups with hexagonal configuration. The optical resonant behavior of the arrays is demonstrated via reflectance spectroscopy. A theoretical prediction of the spectral response, based on rigorous coupled-wave analysis (RCWA), is compared to the experimental observation.

Fabrication

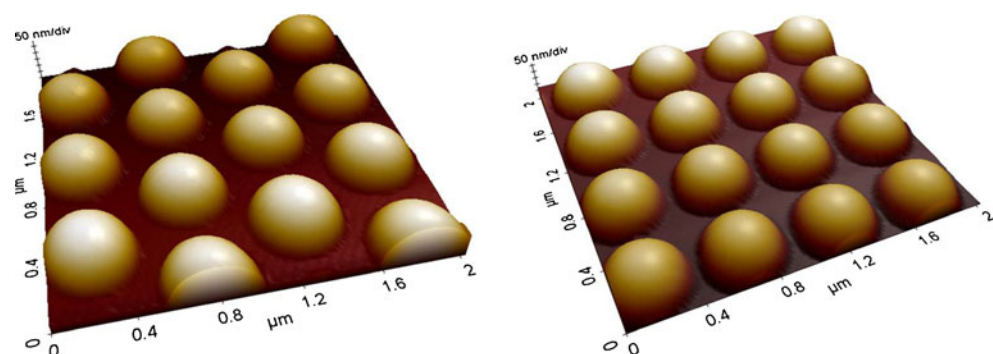
A continuous-wave laser interference system with an exposure wavelength of $\lambda=266$ nm is used to create two-dimensional (2D) structures (i.e., arrays) in photoresist (PR). The periodicity Λ of the resist pattern is given by $\Lambda=\lambda/2\sin\theta$ where θ is the angle of incidence of the incoming light for a symmetric incidence case. The interference system is capable of producing $\sim 100\text{-cm}^2$ periodic patterns with periods down to 200 nm. By controlling the exposure, the fill factor F may vary practically from 0.2 to 0.8, which means that features of ~ 40 nm are obtainable. The samples were characterized with a scanning electron microscope (SEM; JEOL JSM 7600F) and an atomic force microscope (AFM; Park XE-70).

For the experiments, polished 2" Si wafers with a thickness of 370 μm were used as substrates. These were spin-

coated with a positive photoresist (SEPR-701) at 2,000 rpm and cured on a heating plate, adjusted to 110 $^\circ\text{C}$, for 60 s. The thickness of the photoresist film was roughly 280 nm as measured by AFM. After curing, the PR film was exposed with laser interference at an intensity of ~ 0.2 mW/cm 2 . A periodicity of $\Lambda=500$ nm was arbitrarily chosen for the experiments reported. Periodic 2D arrays were achieved through two exposures, in which the second exposure was performed after the sample had been rotated in-plane of either 60° or 90° . Arrays (4×4), each sub-element being 5×5 mm 2 in size, were prepared. The exposure time was 10 s (5 s for each of the two exposures). After a post-baking step on a hot plate at 110 $^\circ\text{C}$ for 1 min, the unexposed PR was removed by rinsing with a developer solution for 1 min. Samples exposed with perpendicular interference fringes resulted in a structure of square-like columns of PR in a rectangular configuration. Exposure with 60° angle, however, yielded a structure of rhombic-like columns in a hexagonal configuration as depicted in Fig. 1a.

Subsequently, a thermal reflow step, where the patterned PR was heated at 190 $^\circ\text{C}$ for either 15 or 20 s, was applied to reshape the structure. For the hexagonal configuration, reflow for 15 s created ellipsoidal-like PR dots while reflow for 20 s generated apparently perfect hemispherical shapes (shown schematically in subpanels b and c of Fig. 1, respectively). For rectangular configurations, both reflow times yielded hemispherical shapes of the PR but of different curvature; the lower reflow time (15 s) gave a smaller

Fig. 2 AFM images of photoresist structures with $\Lambda=500$ nm after reflow at 190 $^\circ\text{C}$ for 20 s (isotropic scales). *Left*: hexagonal configuration. *Right*: rectangular configuration



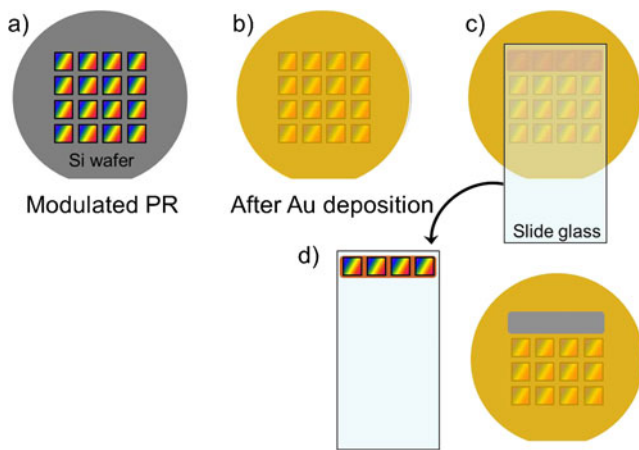


Fig. 3 A schematic of the fabrication process to form arrays of gold nanocup via inverse template process: **a** 4×4 arrays of PR columns on a Si wafer obtained after exposure and developing, **b** after gold deposition, **c** glass slide, glued to the gold film and ejected after curing, **d** dislodged glass slide with 4×1 nano-indented gold films attached to it (right) and its corresponding Si wafer (left)

Table 1 Dimensions of nanocup fabricated by reflow at 190 °C for 20 s

Configuration	Diameter (by SEM), nm	Height (by AFM), nm	Diameter/height
Rectangular	390	185	2.11
Hexagonal	410	197	2.08

diameter-per-height ratio. Smooth and uniform surfaces of hemispherical PR dots in rectangular and hexagonal configurations, reflowed at 190 °C for 20 s, are shown on AFM images in Fig. 2.

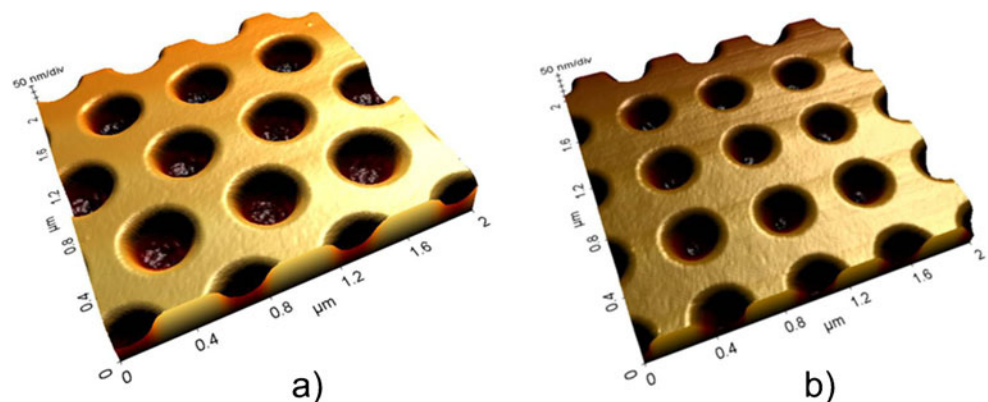
The reflowed PR patterns were used as inverse templates to create the Au nanocup arrays. Approximately 150-nm-thick Au films were deposited by sputtering on top of the PR-patterned Si wafer at a rate of 20 Å/s. A standard 1-mm-thick 3×1 in.² glass microscope slide was then glued to the gold film with epoxy adhesives as depicted in Fig. 3. After curing of the epoxy, the gold film was dislodged by pulling the glass slide off. The procedure is expressed schematically in Fig. 3.

The gold film part, glued to the glass slide, was easily peeled off without any visible residual left on the Si substrate. The PR, remaining in the nanocup's cavities, was removed from the gold film by exposure to oxygen plasma (i.e., ashing) using reactive-ion etching (RIE). It was observed that continuous exposure for 3.5 min at a pressure of 150 mT, power of 200 W, and oxygen flow rate of 50 sccm caused micro-sized cracks in the gold film. Most likely, these micro cracks were caused by overheating of the structure. This was prevented by applying alternating 10-s cycles of plasma for a total of 7 min (with a total on-time of 3.5 min). Cleaning with acetone, instead of RIE, does also work. The nanocup's dimensions are listed in Table 1. From there, we see that the diameter/height ratio is close to the value of 2, which would represent the exact value for a perfect hemisphere. The high structural perfection of the fabricated nanocup is visualized on the AFM images in Fig. 4a, b.

The high level of order is demonstrated in the SEM image in Fig. 5 (only shown for the hexagonal configuration). No irregularities in the periodicity or the physical dimensions are apparent.

Peeling off areas up to 4 cm² was manageable without breaking the substrate. By using thicker substrates and metals instead of the glass slide, we expect that much larger patterned areas can be obtained.

Fig. 4 AFM images of **a** hexagonally and **b** rectangularly arranged gold nanocup (isotropic scales) with $\lambda=500$ nm. The inverse templates (the photoresist pattern) were reflowed at 190 °C for 20 s



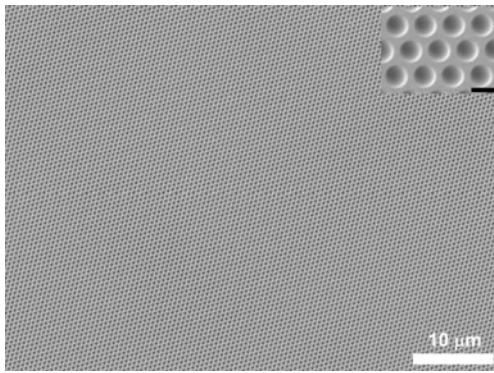


Fig. 5 SEM image of hexagonally arranged gold nanocups with $\Lambda=500$ nm. The inverse template (the photoresist pattern) was reflowed at 190 °C for 20 s. The scale bar on the inset is 500 nm

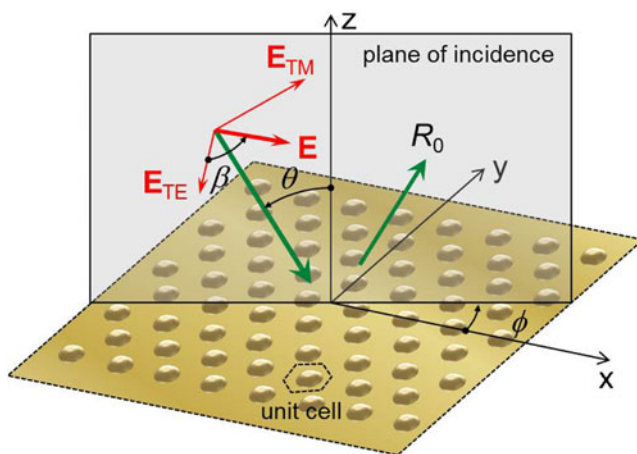
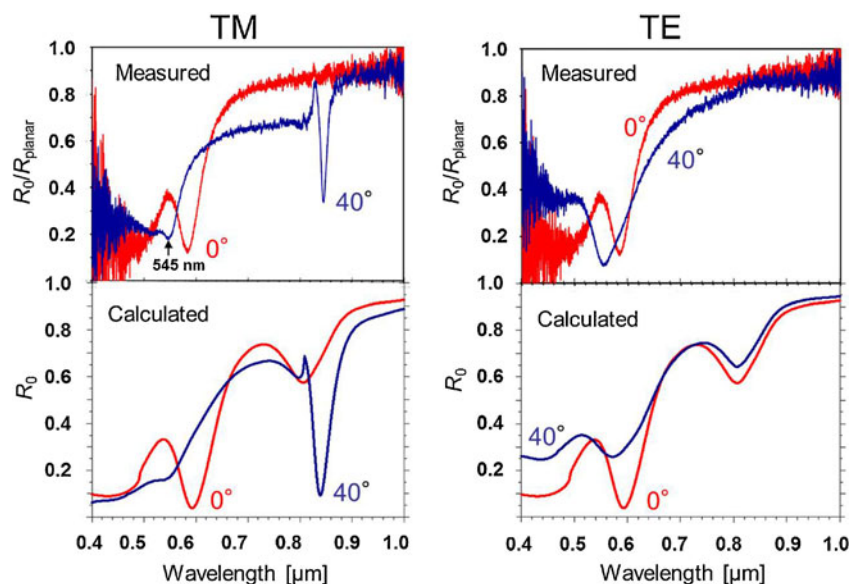


Fig. 6 Relation between incident angles and polarization state of the reflected spectra

Fig. 7 Calculated and normalized experimental reflectance spectra of Au nanocups in rectangular configuration with $\Lambda=500$ nm. Results for two different incident angles ($\theta=0^\circ$ and 40°) of TM-polarized (left) and TE-polarized light (right) are shown



Optical Characterization

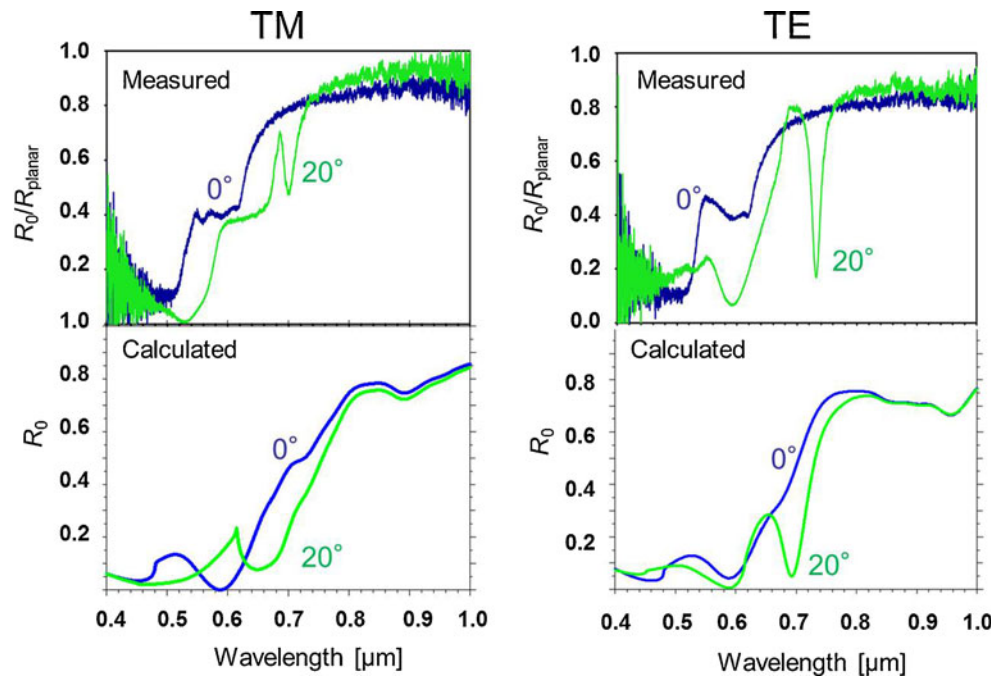
The optical response of the arrays is of interest to determine the fabricated nanostructure qualities. Reflectance spectroscopy in the wavelength interval of $\lambda=400\text{--}1,000$ nm was applied to monitor the plasmonic resonance of the films. A deuterium–tungsten lamp was used as the light source. Zeroth-order reflectance (R_0) spectra were measured at three different incident angles (θ), namely 0° , 20° , and 40° relative to the surface normal axis. The relation between incident angles and polarization states is shown graphically in Fig. 6. The resulting spectra with the intensity of R_0 normalized by the reflectance measured from a planar 200-nm-thick Au film (R_{planar}) are shown in Figs. 7 and 8 for rectangular and hexagonal structures, respectively. A theoretical prediction of the spectral shape is shown for a comparison. We employed a commercial code RSoft DiffractMoD (<http://www.rsoftdesign.com/>) using gold dispersion model given by Rakic et al. [10] to analyze the structures (in 3D) and compute the diffraction efficiencies in reflection. A slice grid size of $0.01\ \mu\text{m}$ and RCWA index resolution (in z direction) of $0.01\ \mu\text{m}$ were used. Resonance features of the transverse magnetic (TM) and transverse electric (TE) modes are apparent as drops in the R_0/R_{planar} intensity occur. These resonance features are due to propagating SPPs induced at the phase-matching condition such that

$$\left| \mathbf{k}_{//} + \frac{2\pi}{\Lambda} (n\mathbf{e}_x + m\mathbf{e}_y) \right| = k_{\text{SP}} \quad (1)$$

where k_{SP} is the propagation constant of the SPP, Λ is the period of the array, and n and m are integers representing diffraction orders.

As shown in Fig. 7, a good qualitative agreement between the theoretical and the experimental data is observed for the

Fig. 8 Calculated and normalized experimental reflectance spectra of Au nanocups in hexagonal configuration with $\Lambda=500$ nm. Results for two different incident angles ($\theta=0^\circ$ and 20°) of TM-polarized (left) and TE-polarized light (right) are shown



rectangular configured structure. This is especially true for the TM-polarized light where even small features such as the dip at 545 nm for 40° incidence is also seen as a small shoulder in the calculated spectra. A sharp resonance line seen at ~ 840 nm for 40° for the TM state is absent for the TE state.

Measured and calculated reflectance spectra of the hexagonally arranged nanocups for 0° and 20° incidence are shown in Fig. 8. In this case, the correlation between the measured and calculated spectra is worse than in Fig. 7. We note that these simulations are performed with the nominal experimental parameters and no attempt has been made to fit these data by parametric variations. A theoretical prediction of the spectral shape, calculated by using RCWA, is shown for a comparison. By optimizing the parameters within experimental tolerances, we expect that better fit can be found; however, this is not the objective of this work.

Conclusions

A method for fabricating photonic devices consisting of strictly periodic arrays of hemispherical nano-indentations in two different configurations was introduced. The method operates at low cost and low complexity but still has high throughput. It is a valuable alternative to prefabricated nanosphere templates commonly used in the production of quasi-ordered nanocups. In particular, we have achieved strictly periodic arrays of Au nanocups in both hexagonal (close packed) and rectangular configuration with simplified processing and measured their spectral response. Analogous processes can be directly implemented in other metals and dielectrics, and they have a considerable potential for upscaling. Our approach, by enabling

the reusability of the substrate and offering flexibility on the substrate choice and nanopattern design, could facilitate the transition of plasmonic technologies to real-world applications in which arrays of strict periodicity are required.

Acknowledgments This research was supported in part by the Energy Research Fund of the National Power Company of Iceland and by the UT System Texas Nanoelectronics Research Superiority Award funded by the State of Texas Emerging Technology Fund. Additional support was provided by the Texas Instruments Distinguished University Chair in Nanoelectronics endowment. We thank Mick Nguyen for assistance with the experiments.

References

1. Maier SA (2007) Plasmonics: fundamentals and applications. Springer Science, New York
2. Love JC et al (2002) Fabrication of wetting properties of metallic half-shells with submicron diameters. *Nano Lett* 2(8):891–894
3. Wang XD et al (2004) Large-scale fabrication of ordered nanobowl arrays. *Nano Lett* 4(11):2223–2226
4. Liu JB et al (2006) A facile route to synthesis of ordered arrays of metal nanoshells with a controllable morphology. *Jpn J Appl Phys* 45(22):L582–L584
5. Xu MJ et al (2009) Fabrication of functional silver nanobowl arrays via sphere lithography. *Langmuir* 25(19):11216–11220
6. Wei X, Chen X, Jiang K (2011) Fabrication of nickel nanostructure arrays via a modified nanosphere lithography. *Nanoscale Res Lett* 6(25)
7. Lu Y et al (2005) Nanophotonic crescent moon structures with sharp edge for ultrasensitive biomolecular detection by local electromagnetic field enhancement effect. *Nano Lett* 5(1):119–124
8. Mirin NA, Halas NJ (2009) Light-bending nanoparticles. *Nano Lett* 9(3):1255–1259
9. Svavarsson HG et al (2011) Fabrication of large plasmonic arrays of gold nanocups using inverse periodic templates. *Plasmonics* 6:741–744
10. Rakic AD et al (1998) Optical properties of metallic films for vertical-cavity optoelectronic devices. *Appl Optics* 37(22):5271–5283